CHEMICAL ENGINEERING TRANSACTIONS
VOL. 50, 2016
A publication of AIDIC
The Italian Association of Chemical Engineering
Online at www.aidic.it/cet
Guest Editors: Katharina Kohse-Höinghaus, Eliseo Ranzi

ISBN 978-88-95608-41-9; **ISSN** 2283-9216
DOI: 10.3303/CET1650013

Dehydration and Dehydrogenation Kinetics of OH Groups in Biomass Pyrolysis

Phillip R. Westmoreland*, Patrick J. Fahey

Department of Chemical and Biomolecular Engineering, North Carolina State University, 911 Partners Way, Raleigh, NC 27695-7905, USA
prwestmo@ncsu.edu

Experiments in pulse-injected flow reactors show that gas-phase pyrolysis of alcohols makes a transition from dehydrogenation dominance for mono-alcohols to dehydration and fragmentation for tested diols and a triol. These dehydration and dehydrogenation reactions are proposed to occur by unimolecular and bimolecular pericyclic reactions, as has been used to explain glucose and cellulose pyrolysis in the absence of ions (Seshadri and Westmoreland, 2012, 2015).
Vaporizable mono-alcohols (ethanol, propanol, butan-2-ol, t-butyl alcohol, and neopentyl alcohol), diols (ethan-1,2-diol, propan-1,2-diol and propan-1,3-diol), and a triol (propan-1,2,3-triol) were pulse-injected into a helium flow, pyrolyzed at 400°C in a tubular flow reactor, and swept directly into a two-dimensional gas chromatograph with time-of-flight mass-spectrometric detection (Pegasus 4D, LECO Corp.). Methanol and 2-propanol were pyrolyzed in a tubular quartz reactor with solely mass-spectrometric analysis.
All the mono-alcohols dehydrogenated except t-butyl alcohol, which has no H on the alcohol carbon. Calculations at a CBS-QB3 level of theory showed that the energetically favored transition states for dehydrogenation were six-centered pericyclic reactions with a hydrogen-bonded ROH molecule. These transition-state enthalpies were about 55 kcal/mol, compared to about 85 kcal/mol for four-centered H_2 elimination. Non-hydrogen-bonded six-centered transition states can occur, but their enthalpies were 109 kcal/mol and higher. The diols displayed dehydrogenation, dehydration, and cyclic Grob fragmentation, and the triol yielded only dehydration and fragmentation products. Details of the analyses are presented, and the findings are compared and contrasted to other findings in the literature.

1. Introduction

Understanding pyrolysis of lignocellulosic biomass requires understanding the roles and fates of hydroxyls (OH groups). Hydroxyls are abundant in cellulose and hemicellulose, present as pendant groups from the rings and in hydroxymethyl groups. Alcohol pyrolysis provides a window into this chemistry.
Computational quantum chemistry has yielded useful new insights into the elementary reactions involved in biomass pyrolysis. Seshadri and Westmoreland (2012, 2015) predicted that OH groups in sugars, cellulose, and hemicelluose can participate both as reactants and as catalysts in pericyclic dehydration and dehydrogenation reactions in the absence of protonation. At about the same time, Mayes and Broadbelt (2012) used quantum calculations to find a dehydration step that eliminates the hydroxymethyl OH on the C6 carbonof cellobiose (di-glucose), forming levoglucosan; Assary and Curtis (2012) found unimolecular and bimolecular pericyclic routes from cellobiose to levoglucosan; and Agarwal et al. (2012) found similar routes with ab-initio molecular dynamics. More recently, Zhou et al. (2014) simulated cellulose pyrolysis using a set of chemically specific reactions and Reactive Monte Carlo, providing additional predictive evidence for the routes.
Alcohol dehydrogenation and dehydration have been studied extensively in the liquid phase and over metal-oxide and organic catalysts, but there has been less study of the gas-phase reactions. To probe the fates of the OH groups experimentally, including their influence on each other, pyrolyses of simple alcohols were conducted with detailed GCxGC-TOFMS analysis of the products. Products were observed corresponding to dehydrogenation, dehydration, and cyclic Grob fragmentation, and mechanistic steps are proposed.

Please cite this article as: Westmoreland P., Fahey P., 2016, Dehydration and dehydrogenation kinetics of oh groups in biomass pyrolysis, Chemical Engineering Transactions, 50, 73-78 DOI: 10.3303/CET1650013

2. Chemicals and apparatus

2.1 Chemicals

Vaporizable mono-alcohols (methanol, ethanol, 1-propanol, 2-propanol, 2-butanol, 2-methylpropan-2-ol, 2,2-dimethylpropan-1-ol, 5-hydroxymethylfurfural, phenol), diols (ethan-1,2-diol, propan-1,2-diol, and propan-1,3-diol), and a triol (propan-1,2,3-triol) were studied. Reactant purities were 99 % or better except for propan-1,3-diol, which was 98 % pure.

2.2 Pyrolysis reactors

A small amount of alcohol (about 0.75 to 0.80 µL) was pulse-injected into a helium flow at the entrance of a 400 °C tubular flow reactor, vaporized, pyrolyzed, and swept through the reactor ($4.5 \bullet 10^{-5}$ mol/s, 0.31 MPa) directly into a two-dimensional gas chromatograph with time-of-flight mass-spectrometric detection (Pegasus 4D, LECO Corp.). The reactor was spliced between the GC's carrier-gas flow controller and the GC's inlet.

The reactor inlet assembly was a 3/8-inch-to-1/4-inch stainless-steel Swagelok® reducer fitting. Inside the tube fitting was a GC septum held in place by a steel washer on the septum's external side. The washer was held in place by a short length of tube swaged into the fitting. This inlet assembly connected to one of two straight runs of a 1/4-inch stainless-steel Swagelok® tee. On the branch of the tee was a 1/4-inch O.D. stainless-steel tube, which supplied helium carrier gas from the GC flow controller. On the 1/4-inch tee's remaining straight run, opposite the reactor inlet, was the reactor entrance.

The reactor was made of a 50-cm length of 1/4-inch O.D. 304SS tube. Its inside wall was coated with ~1/4 micron of amorphous silicon with a silyl-group surface layer (Silcosteel®-Hydroguard," Catalog #22492, Lot #505760-492, Restek Corporation, Bellefonte, Pennsylvania, USA) to prevent transfer lines and vessels from altering the composition of samples containing polar analytes.

Electric heating elements were used for heating the reactor and the transfer line. A small heating tape warmed the carrier gas feed before it reached the branch of the 1/4-inch tee. A rope heater extended from the 1/4-inch tee, along the reactor tube, and along transfer line until reaching the GC inlet, laid directly against the steel tubes in an axial fashion. Three passes of the rope heater extended along the reactor tube, and two passes extended along the transfer line. Thermocouples were placed at the 1/4-inch tee, along the reactor tube at 5, 25, and 45 cm from the entrance of the reactor tube and on the transfer line. Thermocouples were placed directly against the tube but adjacent to the rope heaters, and care was taken to make sure the thermocouples were not between the rope heaters and the tube. This placement was done to ensure the thermocouples measured the tube's temperature and not the heating rope's temperature. Fiberglass insulation webbing was wrapped around the heating elements. The 1-inch-wide webbing was applied in a helical fashion, where each rotation overlapped the previous rotation by 1/2 inch. Two of these helical layers, proceeding in opposite directions, were placed over the reactor tube. One helical layer was placed over the carrier gas feed line, inlet, and transfer line. The fiberglass insulation was subsequently encased by aluminum foil to prevent the fibers from shedding.

Measurements for methanol and 2-propanol were made with pulse injection into a tubular quartz reactor (3.8 mm inner diameter, 3,950 mm^3 heated volume).

2.3 Gas composition analysis

The GCxGC-TOFMS instrument was a Pegasus 4D model from LECO Corporation (Saint Joseph, Michigan, USA), built from an Agilent Technologies GC (Model 7890A, Santa Clara, California, USA). LECO fitted a thermal modulator and a secondary oven to the 7890A GC to enable a GCxGC capability. The entire instrument was operated by LECO Corp.'s ChromaTOF® software. Results were semi-quantitative, as total-ionization signal from hydrocarbons is proportional to the number of carbon atoms in the peak.

The primary column was a 30 m, 0.25 mm inner-diameter, Rtx-200 fused-silica capillary column (polytrifluoropropylmethylsiloxane stationary phase, Restek Corp.) or RTX-2330 (90% bis(cyanopropylsiloxane) / 10% cyanopropylphenylsiloxane, Restek Corp.) with a StabilWax®-DA (Carbowax-20M polyethylene glycol stationary phase, Restek Corp.) secondary column.

For the quartz reactor (methanol and propan-2-ol), gases were analysed with a quadrupole mass spectrometer (MKS Instruments, Model Cirrus^{TM} 2) residual gas analyser. Isomers could not be resolved because of the lack of GC pre-separation, ionization-energy tuning, or better than unit mass resolution. However, unlike in the GCxGC-TOFMS analysis, H_2 could be detected with the QMS.

3. Results

The vaporized alcohols underwent gas-phase pyrolysis, freed from condensed-phase solvent effects and ionic reactions. Surface effects were minimized by the passivated reactor walls. The major and minor products obtained from pyrolysis are shown in Table 1.

Table 1: Reaction products observed from pyrolyzing mono-, di-, and tri-alcohols at 400 °C.

Reactant	Major product(s)	Minor product(s)
methanol, CH_3OH	CH_2=O and (by MS) H_2	CO, CO_2
ethanol, CH_3CH_2OH	CH_3CH=O	C_2H_4, butanal, butanone, but-2-enal
propan-1-ol, $CH_3CH_2CH_2OH$	CH_3CH_2CH=O and (by MS) H_2	CH_3CH=O, C_3H_6 (propene or cyclopropane)
propan-2-ol, $CH_3CH(-OH)CH_3$	$(CH_3)_2$=O	diisopropyl ether, C_3H_6 (propene or cyclopropane)
propan-2-ol d8, $CD_3CD(-OD)CD_3$	$(CD_3)_2$=O	-
butan-2-ol	$CH_3C(=O)CH_2CH_3$	but-2-ene CH_3CH_2=CH_2CH_3
2-methylpropan-2-ol, $(CH_3)_3OH$	2-methylpropene $(CH_3)_2C=CH_2$	-
2,2-dimethylpropan-1-ol, $(CH_3)_3CH_2OH$	2,2-dimethylpropanal $(CH_3)_3CCH$=O, 2-methylpropene $(CH_3)_2C=CH_2$	$(CH_3)_3CH$
5-hydroxymethylfurfural, $HOCH_2$-furan-CH=O	5-formylfurfural O=CH-furan-CH=O	Furfural (furan-CH=O), CH_2=O, furan (cyclic -O-CH=CH-CH=CH-)
---	---	---
ethan-1,2-diol, $HOCH_2CH_2OH$	$HOCH_2CH$(=O), CH_3CH=O, CH_2=O	-
propan-1,2-diol, $HOCH_2CH_2(OH)CH_3$	O=CHCH(=O)CH_3, $HOCH_2CH$(=O)CH_3, CH_3CH_2CH=O, CH_3CH=O, CH_2=O	-
propan-1,3-diol, $HOCH_2CH_2CH_2OH$	CH_3CH_2CH=O, CH_2=CHCH=O, CH_3CH=O, CH_2=O	CH_2=$CHCH_2OH$, $CH_3CH_2CH_2OH$
---	---	---
propan-1,2,3-triol, $HOCH_2CH_2(OH)CH_2OH$	CH_2=CHCH=O, CH_3CH=O, CH_2=O, O=CHC(=O)CH_3, $HOCH_2CH$(=O)CH_3	-

All but one of the saturated primary and secondary mono-alcohols underwent 1,2-dehydrogenation to form a carbonyl group in place of the alcohol group. Primary alcohols formed an aldehyde (methanol formed methanal, ethanol formed ethanol, propanol formed propanal), and secondary alcohols formed a ketone without any change to the alkyl chains (e.g., propan-2-ol formed dimethylketone, butan-2-ol formed methyl ethyl ketone). A mixture of propan-2-ol and its fully deuterated form was pyrolyzed, and there were no products of any H-D exchange, as would have happened if radical chemistry were occurring. The carbonyl compounds were the major products obtained for primary and secondary mono-alcohols, and other products like alkenes created much smaller chromatographic peaks.

The more complicated molecule 5-hydroxymethylfurfural contains a furan ring and carbonyl functionality along with a primary mono-alcohol within its –CH_2OH group. Like the other primary alcohols, it underwent 1,2-dehydrogenation to form 5-formylfurfural (2,5-furandicarboxaldehyde). Some of the 5-hydroxymethylfurfural also deformylated to furfural and formaldehyde.

The main exception to this trend for primary and secondary alkyl mono-alcohols was 2,2-dimethylpropan-1-ol (neopentyl alcohol). It both dehydrogenated to 2,2-dimethylpropanal $(CH_3)_3CCH$=O and dehydrated to 2-methylpropene $(CH_3)_2C=CH_2$.

Two other mono-alcohols were examined that are not primary or secondary alkyl alcohols, and they did react differently. The saturated tertiary mono-alcohol 2-methylpropan-2-ol (t-butyl alcohol) only dehydrated, forming 2-methylpropene, $(CH_3)_2C=CH_2$. Phenol, the aromatic alcohol, did not form any detectable reaction products at 400 °C.

The tested alkyl diols and the triol displayed multiple types of reactions, including 1,2-dehydrogenation and 1,2-dehydration:

- Symmetrical ethan-1,2-diol (ethylene glycol, $HOCH_2CH_2OH$) formed the dehydrogenation product $HOCH_2CH$(=O). It also formed fragment molecules CH_3CH=O and CH_2=O.
- Propan-1,2-diol dehydrogenated to products with a single carbonyl at the internal C-OH position $HOCH_2CH$(=O)CH_3 and with carbonyls at both positions, O=CHCH(=O)CH_3. It also dehydrated the internal C-OH position to form CH_3CH_2CH=O, and it formed the fragment molecules CH_3CH=O and CH_2=O.
- The symmetrical propan-1,3-diol formed some of the 1,2-dehydration product CH_2=$CHCH_2OH$, displaying dehydration at one end, but it formed more CH_2=CHCH=O, which is presumably a subsequent dehydrogenation product. The $CH_3CH_2CH_2OH$ and CH_3CH_2CH=O products imply either re-hydrogenation of

the carbon-carbon double bond or, more likely, a displacement of the hydroxyl. Again, the fragment molecules $CH_3CH{=}O$ and $CH_2{=}O$ are formed.

• Finally, the propan-1,2,3-triol $HOCH_2CH_2(OH)CH_2OH$ forms products that display evidence of dehydration, dehydrogenation, and displacement or re-hydrogenation: $CH_2{=}CHCH{=}O$, $O{=}CHCH(=O)CH_3$, $HOCH_2CH(=O)CH_3$, as well as the $CH_3CH{=}O$ and $CH_2{=}O$ fragment molecules.

4. Discussion

4.1 Role of pericyclic reactions

Pericyclic and radical reactions are the two reaction-route possibilities in the gas phase at 400 °C, where ions, O_2, and d-orbital catalytic chemistry are absent. Both of these reaction types are well suited to study by computational quantum chemistry.

At high enough temperatures, radical chemistry will dominate, initiated by homolytic scission of alcohol molecules into two radicals. These radicals may then undergo decomposition by beta-scission, internal H-abstraction, secondary reaction with the parent alcohol or its products, or combination to make an association product or new products by chemically activated pathways. Such reactions are at the core of radical chain reactions, and they are included in reaction-mechanism generators such as RMG (Green et al., 2005) and EXGAS (Buda et al., 2005; Moss et al., 2008). If radicals are present, their low-activation-energy additions and abstractions dominate the higher-activation-energy pericyclic reactions.

However, pericyclic decompositions (Woodward and Hoffmann, 1970) should dominate at lower temperatures like 400 °C where radicals are presumably absent. Well known examples of pericyclic reactions are the retro-Diels-Alder reaction of cyclohexene, forming 1,3-butadiene + C_2H_2, and the 1,2-dehydrohalogenation and 1,2-dehydration reactions. More recently, catalytic pericyclic reactions of R-OH have been identified by our group (Seshadri and Westmoreland, 2012; Seshadri and Westmoreland, 2015) as crucial for explaining the pyrolysis networks of glucose and cellulose.

4.2 Relevant previous analyses

Unimolecular dehydrations of various alcohols have been studied with computational chemistry. Nimlos et al. (2003) modeled concerted 1,2-dehydrations of pure alcohols with the CBS-QB3 method, finding enthalpies of activation of 67.4, 67.0, 65.9, and 69.6 kcal•mol^{-1} for ethanol, propan-2-ol, 2-methylpropan-2-ol, and ethan-1,2-diol, respectively. Moc et al. (2009) modeled 1-butanol's concerted unimolecular 1,1-, 1,2-, 1,3-, and 1,4-dehydrations and found the four-center 1,2-dehydration to be most favorable energetically, having an activation enthalpy of 67.88 kcal•mol^{-1}. In contrast, the present measurements of mono-alcohol pyrolysis at 400 °C displayed dehydrogenation products.

Propan-1,2,3-triol (glycerol) has received particular attention, computationally and experimentally. Nimlos et al. (2006) calculated the activation energies of its 1,2-dehydrations and 1,3-dehydrations at the CBS-QB3 level of theory. They showed that 1,3-dehydration, which breaks one of propan-1,2,3-triol's carbon-carbon bonds to form methanal, ethenol, and water, is lower in activation energy than the two possible 1,2-dehydrations by 8.0 and 5.7 kcal•mol^{-1}, respectively. Sun et al. (2010) introduced the idea that the initial step could be pericyclic formation of glycidol (2-hydroxymethyl oxirane), and Laino et al. (2011) computed this step to be favored relative to four-center 1,2-dehydration, proceeding on to 3-hydroxypropanal and subsequently to propenal (acrolein) or to methanol (formaldehyde) and ethenol (vinyl alcohol), the latter tautomerizing to ethanal (acetaldehyde). Paine et al. (2007) experimented with pyrolyses of ^{13}C1- and ^{13}C2-labelled propan-1,2,3-triol, and suggested a cyclic 1,3-dehydration (naming it the "cyclic Grob fragmentation") to explain the labelling patterns observed in their methanal and ethanal products. This fragmentation was described as identical to the 1,3-dehydration of Nimlos et al. (2006). Disagreeing, Laino et al. (2011) asserted that Paine's labelling evidence pointed to their glycidol intermediate. The present work detected 3-hydroxypropanal, propenal, ethanal, and methanal, but methylglyoxal $O{=}CHC(=O)CH_3$ instead of glycidol, thus being more consistent with a double 1,2-hydration.

4.3 Analyses of catalyzed vs. uncatalyzed dehydrogenations with computational quantum chemistry

Selected pericyclic dehydrogenations were evaluated using the CBS-QB3 method implemented in Gaussian 09 (Frisch et al., 2009), aiming to explain the behaviour seen in the alcohols. These concerted transition-state structures were considered due to the low activation energies of concerted dehydrations found by Nimlos et al. (2004) and Seshadri and Westmoreland (2012). The unimolecular dehydration and two OH-catalyzed bimolecular dehydrations were evaluated, differing by OH orientation and the loss of H from the alcohol or the alkyl as shown in Figure 1, for methanol, ethanol, 1-propanol, and 2-propanol.

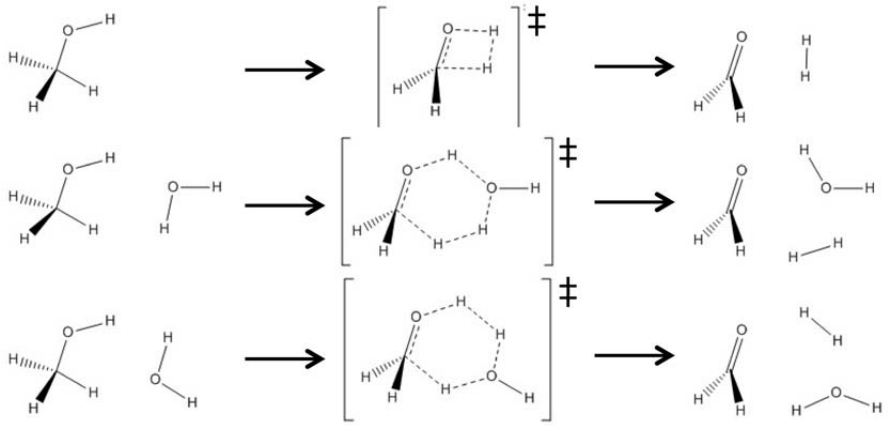

Figure 1: Types of 1,2-dehydrogenation transition states considered, illustrated for methanol: (top) Four-centered, unimolecular; (middle) Six-centered, bimolecular with H_2O's oxygen meta to the alcohol oxygen in the transition-state ring; (bottom) Six-centered, bimolecular with H_2O's oxygen para to the alcohol oxygen.

Table 2: Computed enthalpies of activation (kcal•mol^{-1}) for dehydrogenations and dehydrations.

Mono-alcohol	Dehydrogenation: 4-center	6-center, meta	6-center, para	Dehydration: 4-center	6-center meta
methanol	90.7	59.1	111.4	[makes $^1CH_2$]	
ethanol	85.3	55.4	109.7	66.7	53.2
propan-1-ol	85.8	55.5	110.1	68.1	55.0
propan-2-ol	82.3	53.5	109.9	66.2	52.8

The meta-oxygen, six-center bimolecular dehydrogenation is predicted to be substantially more favorable than the para-oxygen, six-center bimolecular mechanism because its activation enthalpy is roughly 50 kcal•mol^{-1} lower with each of the four separately evaluated monols (Table 2). Note that the catalytic OH need not be in the form of H_2O, but any OH-containing species can supply it, including the other alcohol molecules.
Relative to the four-center, unimolecular dehydrogenation, this meta-oxygen dehydrogenation mechanism has an activation energy strongly favorable by 30 kcal•mol^{-1}. This strong temperature effect and the high initial concentration in the pulse of injected alcohol favor the ROH-catalyzed route, but the bimolecular reaction's lower Arrhenius pre-exponential factor and the low gas density work provide some compensation to the unimolecular route.

4.4 Analyses of catalyzed vs. uncatalyzed dehydrogenations with computational quantum chemistry
Pericyclic dehydrations were analyzed similarly, omitting methanol because its only route is 1,1-dehydration to make singlet CH_2, not an alkene, and omitting the strongly unfavorable para-oxygen route. In the dehydration case, the six-center bimolecular route has a smaller activation-energy advantage and a smaller Arrhenius pre-exponential, so the unimolecular route is generally favoured for gas-phase dehydration.

5. Conclusions

Dehydrogenation was favored over dehydration in gas-phase pyrolysis of primary and secondary mono-alcohols in 400 °C pulse-injection flow-reactor experiments. CBS-QB3 calculations using H_2O as a co-reactant show that the H_2O is regenerated in the dehydrogenation, making it a homogeneous catalyst of the reaction. This reaction has a significant 30 kcal/mol activation-energy advantage over unimolecular H_2 elimination. Furthermore, It is the OH that is catalytic, not water per se, so the alcohol molecules can catalyze each others' dehydrogenation. Dehydration becomes more significant in the experiments on t-butyl alcohol, the diols, and the triol glycerol decompose, and other pericyclic steps consistent with the literature occur in the diol and triol pyrolyses.

Acknowledgments

We gratefully acknowledge financial support by RTI International through subcontract 1-340-0212662 within the National Advanced Biofuel Consortium.

References

Agarwal V., Dauenhauer P.J., Huber G.W., Auerbach S.M., 2012, Ab initio dynamics of cellulose pyrolysis: nascent decomposition pathways at 327 and 600°C, J. Am. Chem. Soc., 134, 14958−14972.

Assary R., Curtiss L., 2012, Thermochemistry and reaction barriers for the formation of levoglucosenone from cellobiose, ChemCatChem, 4, 200-205.

Buda F., Bounaceur R., Warth V., Glaude P.A., Fournet R., Battin-Leclerc F., 2005, Progress towards an unified detailed kinetic model for the autoignition of alkanes from C4 to C10 between 600 and 1200 K. Combust. Flame, 142, 170–186.

Frisch M.J., Trucks G.W., Schlegel H.B., Scuseria G.E., Robb M.A., Cheeseman J.R., Scalmani G., Barone V., Mennucci B., Petersson G.A., Nakatsuji H., Caricato M., Li X., Hratchian H.P., Izmaylov A.F., Bloino J., Zheng G., Sonnenberg J.L., Hada M., Ehara M., Toyota K., Fukuda R., Hasegawa J., Ishida M., Nakajima T., Honda Y., Kitao O., Nakai H., Vreven T., Montgomery Jr. J. A., Peralta J.E., Ogliaro F., Bearpark M., Heyd J.J., Brothers E., Kudin K.N., Staroverov V.N., Keith T., Kobayashi R., Normand J., Raghavachari K., Rendell A., Burant J.C., Iyengar S.S., Tomasi J., Cossi M., Rega N., Millam J.M., Klene M., Knox J.E., Cross J.B., Bakken V., Adamo C., Jaramillo J., Gomperts R., Stratmann R.E., Yazyev O., Austin A.J., Cammi R., Pomelli C., Ochterski J.W., Martin R.L., Morokuma K., Zakrzewski V.G., Voth G.A., Salvador P., Dannenberg J.J., Dapprich S., Daniels A.D., Farkas O., Foresman J.B., Ortiz J.V., Cioslowski J., Fox D.J., 2013, Gaussian 09, Revision D.01, Gaussian, Inc., Wallingford CT.

Green W.H., Allen J.W., Buesser B.A., Ashcraft R.W., Beran G.J., Class C.A., Gao C., Goldsmith C.F., Harper M.R., Jalan A., Keceli M., Magoon G.R., Matheu D.M., Merchant S.S., Mo J.D., Petway S., Raman S., Sharma S., Song J., Suleymanov Y., Van Geem K.M., Wen J., West R.H., Wong A., Wong H.-W., Yelvington P.E., Yee N., Yu J., 2013, RMG - Reaction Mechanism Generator v4.0.1 <http://rmg.sourceforge.net/> accessed 04.01.2016.

Laino T., Tuma C., Curioni A., Jochnowitz E., Stolz S., 2011, A revisited picture of the mechanism of glycerol dehydration, J Phys Chem A, 115, 3592-3595.

Mayes H.B., Broadbelt L.J., 2012, Unraveling the reactions that unravel cellulose, J. Phys. Chem. A, 116, 7098-7106.

Moc J., Simmie J.M., Curran H.J., 2009, The elimination of water from a conformationally complex alcohol: A computational study of the gas phase dehydration of n-butanol, J. Molecular Structure, 928.

Moss J.T., Berkowitz A.M., Oehlschlaeger M.A., Biet J., Warth V., Glaude P.A., Battin-Leclerc F., 2008, An experimental and kinetic modeling study of the oxidation of the four isomers of butanol. J Phys Chem A, 112, 10843–10855.

Nimlos M.R., Blanksby S.J., Ellison G.B., Evans R.J., 2004, Enhancement of 1,2-dehydration of alcohols by alkali cations and protons: a model for dehydration of carbohydrates, J. Analyt. Appl. Pyrolysis, 66, 3-27.

Nimlos M.R., Blanksby S.J., Qian X., Himmel M.E., Johnson D.K., 2006, Mechanisms of Glycerol Dehydration, J. Phys. Chem. A, 110, 6145-6156.

Paine III J.B., Pithawalla Y.B., Naworal J.D. Thomas Jr. C.D., 2007, Carbohydrate pyrolysis mechanisms from isotopic labeling Part 1: The pyrolysis of glycerin: Discovery of competing fragmentation mechanisms affording acetaldehyde and formaldehyde and the implications for carbohydrate pyrolysis, J. Analyt. Appl. Pyrolysis, 80, 297-311.

Seshadri V., Westmoreland P.R., 2012, Concerted reactions and mechanism of glucose pyrolysis and implications for cellulose kinetics, J. Phys. Chem. A, 116, 11997-20013.

Seshadri V., Westmoreland P.R., 2015, Roles of hydroxyls in the noncatalytic and catalyzed formation of levoglucosan from glucose, Catalysis Today, In Press, DOI: 10.1016/j.cattod.2015.10.033

Woodward R.W., Hoffmann R., 1970, The Conservation of Orbital Symmetry. Verlag Chemie GmbH, Weinheim Germany.

Zhou X., Nolte M.W., Mayes H.B., Shanks B.H., Broadbelt L.J., 2014, Experimental and mechanistic modeling of fast pyrolysis of neat glucose-based carbohydrates. 1. Experiments and development of a detailed mechanistic model, Ind. Eng. Chem. Res., 53, 13274-13289.